
Subspace Networks for Few-shot Classification

Arnout Devos
EPFL
arnout.devos@epfl.ch

Matthias Grossglauser
EPFL
matthias.grossglauser@epfl.ch

Abstract

We propose *subspace networks* for the problem of few-shot classification, where a classifier must generalize to new classes not seen in the training set, given only a small number of examples of each class. Subspace networks learn an embedding space in which classification can be performed by computing distances of embedded points to subspace representations of each class. The class subspaces are spanned by examples belonging to the same class, transformed by a learnable embedding function. Similarly to recent approaches for few-shot learning, subspace networks reflect a simple inductive bias that is beneficial in this limited-data regime and they achieve excellent results. In particular, our proposed method shows consistently better performance than other state-of-the-art few-shot distance-metric learning methods when the embedding function is deep or when training and testing domains are shifted.

1 Introduction

The ability to adapt quickly to new situations is a cornerstone of human intelligence. When given a previously unseen task, humans can use their previous experience and learning abilities to perform well on this new task in a matter of seconds and with a relatively small amount of new data. Artificial learning methods have been shown to be very effective for specific tasks, often surpassing human performance (Silver et al. [2016], Esteva et al. [2017]). However, by relying on standard training paradigms for supervised learning or reinforcement learning, these artificial methods still require much training data and training time to adapt to a new task.

An area of machine learning that learns and adapts from a small amount of data is called *few-shot learning* (Fei-Fei et al. [2006]). A *shot* corresponds to a single example, e.g., an image and its label. In few-shot learning the learning scope is expanded from the classic setting of a single task with many shots to a variety of tasks with a few shots each. In the case of classification, an "*N*-way *K*-shot" task is composed of a labeled *support set* with *K* shots for each of the *N* classes, and a *query set* with unlabeled test examples. Several machine learning approaches have been developed to study learning from limited examples, including generative models (Fei-Fei et al. [2006], Lake et al. [2015]), meta-learning (Finn et al. [2017], Ravi and Larochelle [2017]), and distance-metric learning (Vinyals et al. [2016], Snell et al. [2017], Sung et al. [2018]).

Chen et al. [2019] showed that a distance-metric learning based method called *prototypical networks* (Snell et al. [2017]), although simple in nature, achieves competitive performance with state-of-the-art meta-learning and other distance-metric learning methods across multiple datasets. Distance-metric learning methods approach the few-shot classification problem by "*learning to compare*". Intuitively, when a model can tell the similarity between two inputs, then it can classify an unseen input based on its similarity to previously seen instances (Koch et al. [2015]). To learn high capacity nonlinear comparison models, most modern few-shot distance-metric learning methods make use of an embedding space to measure distance. Such an embedding space is obtained through an embedding function, e.g., a deep neural network.

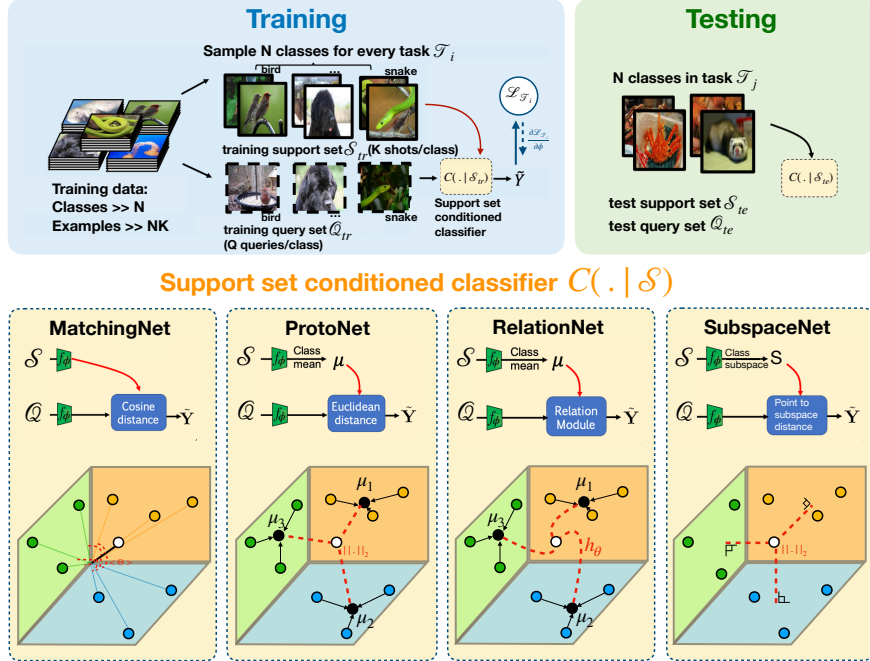


Figure 1: Distance-metric learning based methods for few-shot classification with \mathcal{S} the support set (colored circles), \mathcal{Q} the query set (white circle), \tilde{Y} the output distribution over classes for the query points, f_ϕ a neural network based embedding function, and h_θ a neural network based distance function for RelationNet. Figure inspired by Chen et al. [2019].

There are different state-of-the-art few-shot methods that employ a distance metric for classification. MatchingNet (Vinyals et al. [2016]) computes the average cosine distance of the query example to every support example of each class. ProtoNet (Snell et al. [2017]) compares the Euclidean distance between the query example and the class mean of embedded support examples. RelationNet (Sung et al. [2018]) also relies on the embedded class mean, but replaces the fixed distance metric with a learnable CNN relation module.

Since there is very few data available, a classifier should have a simple inductive bias (Snell et al. [2017]). Our approach, *subspace networks*, is based on the idea that there exists an embedding in which points from the same class lie close to its subspace representation. In order to do this, we learn a nonlinear mapping of the input space to an embedding space by using a neural network and construct a subspace representation for each class with the examples of the support set in the embedding space. Classification of an embedded query point is then performed by simply finding the nearest class subspace. Subspaces have been used to model images for decades in computer vision and machine learning. For example, the Linear Regression Classification method by Naseem et al. [2010] relies on the fact that the set of all reflectance functions produced by Lambertian objects, which parts of natural images are composed of, lie near a low-dimensional linear subspace (Basri and Jacobs [2003]). Figure 1 shows an overview of the few-shot learning process and a comparison of the proposed method with other distance-metric learning based approaches.

2 Subspace Networks

2.1 Notation

We formulate the N -way K -shot classification problem in an episodic way. A dataset is composed of many N -way K -shot episodes or tasks. Every episode has a small support set of N classes with K labeled examples each $\mathcal{S} = \{(\mathbf{x}_{11}, y_{11}), \dots, (\mathbf{x}_{NK}, y_{NK})\}$, and a larger query set of Q different examples for each of those N classes $\mathcal{Q} = \{(\mathbf{x}_{11}, y_{11}), \dots, (\mathbf{x}_{NQ}, y_{NQ})\}$. Note that the query set contains labels only during training, and the objective is to predict the labels of the query set during

testing. In the support set \mathcal{S} and query set \mathcal{Q} each $\mathbf{x}_{ij} \in \mathbb{R}^D$ is the D -dimensional feature vector of an example and $y_{ij} \in \{1, \dots, N\}$ is the corresponding label.

2.2 Model

Subspace networks construct a K -dimensional embedded subspace \mathbf{S}_n of each class n , given K shots per class, through an embedding function $f_\phi : \mathbb{R}^D \rightarrow \mathbb{R}^M$ with learnable parameters ϕ . With slight abuse of notation, every class is represented by its subspace matrix $\mathbf{S}_n \in \mathbb{R}^{M \times K}$, that is composed of the K vectors of the embedded class support points:

$$\mathbf{S}_n = [f_\phi(\mathbf{x}_{n1}) \quad \dots \quad f_\phi(\mathbf{x}_{nK})] \quad (1)$$

The *point-to-subspace distance* $\tilde{d}(\mathbf{e}_i, \mathbf{S}_n)$ of a point $\mathbf{e}_i \in \mathbb{R}^M$ in the embedding space to a class subspace \mathbf{S}_n can be measured by constructing the closest point in the subspace in terms of a certain distance metric. The closest point can be constructed with a linear combination (represented by vector $\mathbf{a} \in \mathbb{R}^{K \times 1}$) of the embedded support examples spanning that space. By using a Euclidean distance metric, this can be formulated as a quadratic optimization problem in \mathbf{a} of the following form:

$$\tilde{d}(\mathbf{e}_i, \mathbf{S}_n) = \min_{\mathbf{a}} d(\mathbf{e}_i, \mathbf{S}_n \mathbf{a}) = \min_{\mathbf{a}} \|\mathbf{e}_i - \mathbf{S}_n \mathbf{a}\|_2 \quad (2)$$

The associated learning problem with this few-shot (K) high-dimensional (M) overdetermined system is *least-squares linear regression*. Given that $M \geq K$, this is a well conditioned system, and it admits a *differentiable* closed-form solution (Friedman et al. [2001])

$$\tilde{d}(\mathbf{e}_i, \mathbf{S}_n) = \left\| \mathbf{e}_i - \mathbf{S}_n (\mathbf{S}_n^T \mathbf{S}_n)^{-1} \mathbf{S}_n^T \mathbf{e}_i \right\|_2 \quad (3)$$

$$= \|\mathbf{e}_i - \mathbf{P}_n \mathbf{e}_i\|_2 \quad (4)$$

where it is important to note that the matrix to be inverted is of size $K \times K$ and the number of shots K is usually small. The transformation matrix \mathbf{P}_n projects the point \mathbf{e}_i orthogonally onto the subspace spanned by the columns of \mathbf{S}_n , which follows from the following theorem in Koç and Barkana [2014]:

Theorem 1. *The transformation matrix \mathbf{P}_n of the n^{th} class with subspace matrix \mathbf{S}_n and the projection matrix onto the column space of \mathbf{Q}_n , where $\mathbf{S}_n = \mathbf{Q}_n \mathbf{R}_n$ is the QR-factorization of \mathbf{S}_n , are the same, that is, $\mathbf{P}_n = \mathbf{Q}_n \mathbf{Q}_n^T$.*

Note that this transformation matrix \mathbf{P}_n has to be computed only for every class, not every example, which speeds up practical computation. Because the embedding function f_ϕ can output linearly dependent embeddings for different support examples, a small term $\lambda > 0$ is added to avoid singularity:

$$\tilde{d}(\mathbf{e}_i, \mathbf{S}_n) = \left\| \mathbf{e}_i - \mathbf{S}_n (\mathbf{S}_n^T \mathbf{S}_n + \lambda \mathbf{I})^{-1} \mathbf{S}_n^T \mathbf{e}_i \right\|_2 \quad (5)$$

Given such a point-to-subspace distance function $\tilde{d} : \mathcal{R}^M \times \mathcal{R}^{M \times K} \rightarrow [0, +\infty)$, subspace networks produce a distribution over classes for a query point \mathbf{x} based on a softmax over distances to each of the class subspaces in the larger embedding space:

$$p_\phi(y = n \mid \mathbf{x}) = \frac{\exp\left(-\tilde{d}(f_\phi(\mathbf{x}), \mathbf{S}_n)\right)}{\sum_{n'} \exp\left(-\tilde{d}(f_\phi(\mathbf{x}), \mathbf{S}_{n'})\right)} \quad (6)$$

Learning continues by minimizing the negative log-probability function $\mathcal{L}(\phi) = -\log p_\phi(y = n \mid \mathbf{x})$ of the true class n via Stochastic Gradient Descent (SGD). Training episodes/tasks are formed by randomly sampling a subset of N classes from the training set. Then, a subset of K examples within each class is chosen to act as the support set \mathcal{S} , and a subset of Q examples within each class is chosen to act as the query set \mathcal{Q} . Algorithm 1 contains a detailed version of the subspace networks training procedure.

Algorithm 1 Subspace Networks

Require: Training set with N -way K -shot episodes/tasks $\{\mathcal{T}_1, \dots, \mathcal{T}_{N_T}\}$, with every \mathcal{T}_i containing sets $\mathcal{S}_{\mathcal{T}_i} = \{(\mathbf{x}_{i11}, y_{i11}), \dots, (\mathbf{x}_{iNK}, y_{iNK})\}$ and $\mathcal{Q}_{\mathcal{T}_i} = \{(\mathbf{x}_{i1Q}, y_{i1Q}), \dots, (\mathbf{x}_{iNQ}, y_{iNQ})\}$. $\mathcal{S}_{\mathcal{T}_i n}$ and $\mathcal{Q}_{\mathcal{T}_i n}$ denote the class n subsets of support and query sets, respectively, of episode \mathcal{T}_i .

Require: α, λ : step size and conditioning parameters

- 1: Randomly initialize ϕ
- 2: **while** not done **do**
- 3: **for** i in $\{1, \dots, N_T\}$ **do**
- 4: **for** n in $\{1, \dots, N\}$ **do**
- 5: $\mathbf{S}_n \leftarrow f_\phi(\mathcal{S}_{\mathcal{T}_i n})$ \triangleright Embed class support set subspace $\mathbf{S}_n \in \mathbb{R}^{M \times K}$
- 6: $\mathbf{P}_n \leftarrow \mathbf{S}_n (\mathbf{S}_n^T \mathbf{S}_n + \lambda \mathbf{I})^{-1} \mathbf{S}_n^T$ \triangleright Compute transformation matrix $\mathbf{P}_n \in \mathbb{R}^{M \times M}$
- 7: **end for**
- 8: $\mathcal{L}_{\mathcal{T}_i} \leftarrow 0$ \triangleright Initialize episode loss
- 9: **for** n in $\{1, \dots, N\}$ **do**
- 10: **for** $(\mathbf{x}, y = n)$ in $\mathcal{Q}_{\mathcal{T}_i n}$ **do**
- 11: $\mathcal{L}_{\mathcal{T}_i} \leftarrow \mathcal{L}_{\mathcal{T}_i} + \frac{1}{NQ} \left[\|f_\phi(\mathbf{x}) - \mathbf{P}_n f_\phi(\mathbf{x})\|_2 + \log \sum_{n'} \exp(-\|f_\phi(\mathbf{x}) - \mathbf{P}_{n'} f_\phi(\mathbf{x})\|_2) \right]$
- 12: **end for**
- 13: **end for**
- 14: **end for**
- 15: $\phi \leftarrow \phi - \alpha \nabla_\phi \sum_i \mathcal{L}_{\mathcal{T}_i}$ \triangleright Update embedding parameters ϕ with gradient descent
- 16: **end while**

3 Experiments

In terms of few-shot learning datasets, we focused on the image-based mini-ImageNet (Vinyals et al. [2016]) and CUB-200-2011 (Wah et al. [2011]), hereafter referred to as *CUB*, instead of Omniglot (Lake et al. [2011]) because the former ones are more challenging, and the error rate is more sensitive to model improvements. In addition to the intrinsic intra-domain difference of the classes within these datasets, we also performed experiments to evaluate the performance of our method under domain shift. To this end, we combine these datasets to form a mini-ImageNet \rightarrow CUB (train \rightarrow test) experiment as in Chen et al. [2019], and we propose a new CUB \rightarrow mini-ImageNet experiment.

In this section, we address the following research questions: (i) How does the performance of subspace networks scale when the embedding function becomes deeper? (Section 3.2). (ii) Can subspace networks benefit from more shots? (Section 3.2). (iii) Is there a difference in performance between datasets with different class divergences? (Sections 3.2 and 3.3). (iv) How well do learned subspace networks transfer from one dataset to another (domain-shift)? (Section 3.3).

3.1 Experimental Setup and Datasets

The mini-Imagenet dataset proposed by Vinyals et al. [2016] contains 100 classes, with 600 84×84 images per class sampled from the larger ImageNet dataset (Deng et al. [2009]). Following Ravi and Larochelle [2017], 64 classes are isolated for the training set and, from the remaining classes, the validation and test sets of 16 and 20 classes, respectively, are constructed. We use exactly the same train/validation/test split of classes as the one suggested by Ravi and Larochelle [2017]. The CUB dataset contains 200 classes of birds and 11,788 images in total. Following Hilliard et al. [2018], we randomly split the CUB dataset into 100 train, 50 validation, and 50 test classes.

To ensure a fair comparison with other distance-metric based methods, we perform experiments under the same conditions using the verified re-implementation of MatchingNet (Vinyals et al. [2016]), ProtoNet (Snell et al. [2017]) and RelationNet (Sung et al. [2018]) by Chen et al. [2019]. We decide to compare with these methods in particular, because they serve as the basis of many state-of-the-art few-shot classification algorithms (Oreshkin et al. [2018], Xing et al. [2019]), and our method is easily interchanged with them. We implement subspace networks using the automatic-differentiation framework PyTorch (Paszke et al. [2017]) and make our code publicly available online ¹.

¹<http://www.github.com/ArnoutDevos/SubspaceNet>

Implementation details. Three different feature embedding architectures are used throughout our experiments. The *Conv-4* backbone is composed of four convolutional blocks with an input size of 84×84 as in Snell et al. [2017]. Each block comprises a 64-filter 3×3 convolution with a padding of 1 and a stride of 1, a batch normalization layer, a ReLU nonlinearity and a 2×2 max-pooling layer. The *ResNet-10* backbone has an input size of 224×224 and is a simplified version of ResNet-18 in He et al. [2016], by using only one residual building block in each layer. *ResNet-34* is the same as described in He et al. [2016].

All methods are trained with a random parameter initialization and use the Adam optimizer (Kingma and Ba [2014]) with an initial learning rate of 10^{-3} . During the training stage, data augmentation is done in the form of: random crop, color jitter, and left-right flip. For MatchingNet, a rather sophisticated long-short term memory (LSTM)-based full context embedding (FCE) classification layer without fine-tuning is used over the support set, and the cosine similarity metric is multiplied by a constant factor of 100. In RelationNet, the L2 norm is replaced with a softmax layer to help the training procedure. The relation module is composed of 2 convolutional blocks (same as in Conv-4), followed by two fully connected layers of size 8 and 1.

In all settings, we train for 60,000 episodes and use the held-out validation set to select the best model during training. To construct an N -way episode, we sample $N = 5$ classes from the training set of classes. From each sampled class, we sample K examples to construct the support set of an episode and $Q = 16$ examples for the query set. During testing, we average the results over 600 episodes of exactly the same form, but this time they are sampled from the test set. Many training optimizations exist, including using more classes in the training episodes than in the testing episodes (Snell et al. [2017]) or pre-training the feature extractor with all training classes and a linear output layer (Qiao et al. [2018]). However, we train all methods from scratch and construct our training and testing episodes to have the same number of classes N and shots K because we are interested in the relative performance of the methods. For SubspaceNet, the conditioning parameter used to ensure a fully invertible matrix in Equation 5 is set to $\lambda = 10^{-3}$.

Despite the modification of some implementation details of the methods with respect to the original papers, using these settings ensures a fair comparison and Chen et al. [2019] report a maximal drop in classification performance of 2% with respect to the original reported performance of each method.

3.2 Few-shot Classification: mini-ImageNet and CUB

To evaluate the few-shot image classification performance, we use the mini-ImageNet and CUB datasets. Figure 2 shows the results for 5-way classification for both datasets on backbones of different depth and for a different number of shots.

First, we address the effect of the feature embedding backbone depth. As expected, performance of the few-shot classification methods generally improves when a deeper backbone is used. As can be seen, the relative rank in terms of classification accuracy of the distance-metric based methods shifts significantly when going from the Conv-4 embedding architecture to a deeper ResNet-10 or ResNet-34. For example in Figure 2(d), RelationNet performs best in the Conv-4 setting, but worst when using ResNet-34 and SubspaceNet takes first place. Generally, across datasets and number of shots, subspace networks outperform the other methods when the backbone is relatively deep (ResNet-10 and deeper).

Secondly, because subspace networks are expected to build a better subspace representation when more support examples are available per class, we investigate the effect of the number of shots. As expected, when increasing the number of shots K per class, the classification accuracies increase for almost all methods. Interestingly, even for the smaller Conv-4 backbone, subspace networks outperform all other methods on both datasets when 10 shots are used.

Lastly, comparing the classification results on the CUB and mini-ImageNet datasets, the accuracies are consistently higher for CUB under the same setting (backbone, shots, method). This can be explained by the difference in divergence of classes; this difference is higher in mini-ImageNet than in CUB (Chen et al. [2019]). Section 3.3 discusses extra experiments on the transferrability of different methods under domain-shift and further reports on the difference in divergence between classes in CUB and mini-ImageNet.

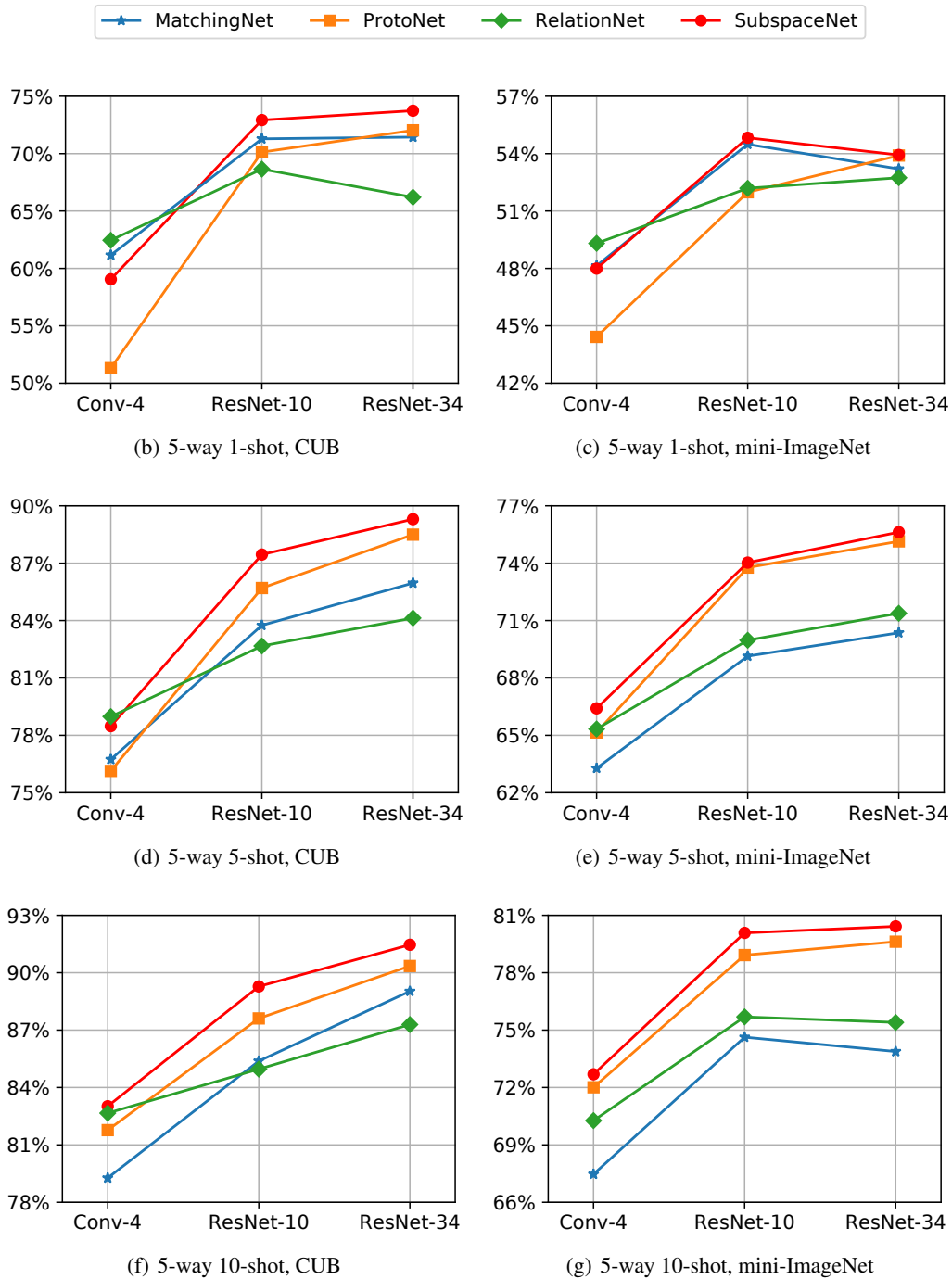


Figure 2: 5-way few-shot classification accuracies in function of backbone depth on the CUB and mini-ImageNet datasets. Subspace networks outperform all other distance-metric based methods, using relatively deep backbones (ResNet-10 and ResNet-34). 1-shot accuracies for methods other than SubspaceNet taken from Chen et al. [2019]. (See Appendix A for tables with numerical accuracies and 95% confidence intervals.)

Table 1: Identical domain and domain shift accuracies for 5-way 5-shot classification using a ResNet-10 backbone and mini-ImageNet and CUB datasets. The best-performing method is highlighted.

| training set | CUB | mini-ImageNet | mini-ImageNet | CUB |
|---------------------------|---------------------|---------------------|---------------------|---------------------|
| test set | CUB | mini-ImageNet | CUB | mini-ImageNet |
| MatchingNet | 83.75 ± 0.60 | 69.14 ± 0.69 | 52.59 ± 0.71 | 48.95 ± 0.67 |
| ProtoNet | 85.70 ± 0.52 | 73.77 ± 0.64 | 59.22 ± 0.74 | 53.58 ± 0.73 |
| RelationNet | 82.67 ± 0.61 | 69.97 ± 0.68 | 54.36 ± 0.71 | 45.27 ± 0.66 |
| SubspaceNet (ours) | 87.45 ± 0.48 | 74.03 ± 0.68 | 62.71 ± 0.71 | 56.66 ± 0.68 |

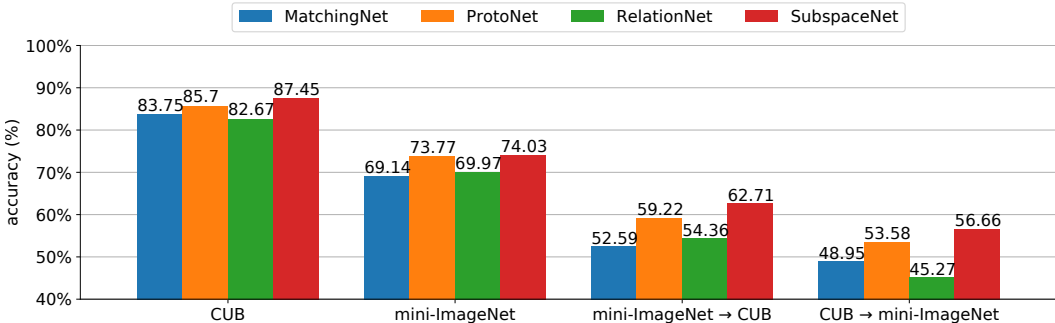


Figure 3: 5-way 5-shot classification accuracies in different scenarios with a ResNet-10 backbone. Two datasets with different class granularity are used: *CUB* (all birds) and *mini-ImageNet* (cars, animals, objects, ...). From left to right there is an increasing class/domain shift between training and test sets, first in an intra-dataset setting and last in an inter-dataset setting. SubspaceNet achieves the highest accuracy in all settings. (See Table 1 for detailed statistics and 95% confidence intervals.)

3.3 Domain Shift: mini-ImageNet → CUB and CUB → mini-ImageNet

We evaluate how the distance-metric based few-shot classification methods perform when the test set is increasingly different from the train set. In addition to the evaluations on mini-ImageNet and CUB separately in Section 3.2, in this section we perform experiments by changing the training and testing domain from one dataset to another (denoted as *train* → *test*). The mini-ImageNet → CUB setting, introduced by Chen et al. [2019], represents a coarse-grained train set to fine-grained test set domain-shift. Conversely, we propose to use the inverse scenario CUB → mini-ImageNet as well.

In mini-ImageNet → CUB, all 100 classes from mini-ImageNet make up the training set and the same 50 validation and 50 test classes from CUB are used. Conversely, in CUB → mini-ImageNet, all 200 classes from CUB make up the training set and the same 16 validation and 20 test classes from mini-ImageNet are used. To illustrate the domain shift, we can look at the mini-ImageNet → CUB setting: the 200 classes of CUB are all types of birds, whereas the 64 classes in the training set of mini-ImageNet only contain 3 types of birds, which are not to be found in CUB. Evaluating the domain-shift scenario enables us to understand better which method is more general.

Table 1 and Figure 3 present our results in the context of existing state-of-the-art distance-metric learning based methods. All experiments in this setting are conducted with a ResNet-10 backbone on a 5-way 5-shot problem. The intra-domain difference between classes is higher in mini-ImageNet than in CUB (Chen et al. [2019]), which is reflected by a drop of the test accuracies of all methods. It can also be seen that when the domain difference between the training and test stage classes increases (left to right in Figure 3) the performance of all few-shot algorithms lowers.

As expected, the classification accuracy lowers slightly when going from the mini-ImageNet → CUB to the CUB → mini-ImageNet setting. Interestingly though, it does not decrease substantially. This shows that the different feature embeddings generalize well, at least across these two different datasets. Compared to other distance-metric learning based methods, subspace networks show significantly better performance in both the mini-ImageNet → CUB setting and CUB → mini-ImageNet setting.

4 Related work

In addition to the reproduced distance-metric learning based few-shot methods, there is a large body of work on few-shot learning and distance-metric learning. We discuss work that is more closely related to subspace networks in particular.

Our approach shows many similarities to the linear regression classification (LRC) method by Naseem et al. [2010], where each class is represented by the subspace spanned by its examples. This approach was developed for face recognition, where only a few examples are available, however it relies on a linear embedding. Our approach also uses few examples, but it incorporates neural networks in order to nonlinearly embed examples and we couple this with episodic training to handle the few-shot scenario.

Bertinetto et al. [2018] propose to use regularized linear regression as a classifier on top of the embedding function. Doing so, they directly approach a classification problem with a regression method, but they show competitive results. To achieve this, they introduce learnable scalars that scale and shift the regression outputs for them to be used in the cross-entropy loss. Subspace networks rely on the same closed-form solver for linear regression to compute the projection matrices, but are inherently designed for classification problems because of their similarity to the LRC method (Naseem et al. [2010]).

Meta-learning is another popular approach for few-shot learning and generalizes naturally to few-shot regression and reinforcement learning problems. Ravi and Larochelle [2017] use an external LSTM to learn to optimize parameters of a model, given the gradients of those parameters. Model-agnostic meta-learning (MAML) by Finn et al. [2017] outperforms the LSTM-based method by using a meta-gradient over multiple individual episode gradient update steps. Our subspace networks method can also be seen as a form of meta-learning, in the sense that it dynamically produces a simple classifier from incoming test episodes, yet the parametrized embedding function f_ϕ remains fixed after training.

Oreshkin et al. [2018] show that, following Hinton et al. [2015], by adding a learnable temperature α in the softmax ($p_{\phi,\alpha}(y = n|\mathbf{x}) = \text{softmax}(-\alpha d(\mathbf{e}_i, \mathbf{P}_n \mathbf{e}_i))$), they enable the model to learn the best regime for each similarity metric. By using such a learnable temperature, the performance difference between matching networks and prototypical networks vanishes. However, the performance of prototypical networks improves only slightly. Also, the idea to make the embedding function conditionally dependent on the support set (Vinyals et al. [2016]) is used in the form of conditional batch normalization by Oreshkin et al. [2018]. They show that by combining support-set conditioned batch normalization with temperature learning, impressive performance gains can be achieved.

Concurrently, similar work by Simon et al. [2019] explores subspace representations for few-shot learning. In contrast to our least squares linear regression approach, they make use of a truncated singular value decomposition (SVD) of the support example matrix, where the mean is subtracted from each embedded example. Although singular values and right-singular vectors are computed, only the left-singular vectors are relevant, rendering the approach less elegant compared to ours. Due to subtraction of the mean, their method does not work in the 1-shot setting.

5 Conclusion

We have proposed a simple method called subspace networks for few-shot classification; the method is based on the idea that we can represent each class by the subspace spanned by its examples in a representation space learned by a neural network. Using episodic training, we train these networks to perform well specifically in the few-shot setting. Even without sophisticated extensions, the approach produces better results than other state-of-the-art distance-metric learning based methods, especially when the neural feature extractor architecture is relatively deep. We further demonstrate that subspace networks achieve superior performance in the case of domain shift. A natural direction for future work is to study the effect of using a low-rank approximation of the subspace. Overall, the simplicity and effectiveness of subspace networks makes it a promising approach for distance-metric based few-shot classification.

References

- Ronen Basri and David W Jacobs. Lambertian reflectance and linear subspaces. *IEEE Transactions on Pattern Analysis & Machine Intelligence*, (2):218–233, 2003.
- Luca Bertinetto, Joao F Henriques, Philip HS Torr, and Andrea Vedaldi. Meta-learning with differentiable closed-form solvers. *arXiv preprint arXiv:1805.08136*, 2018.
- Wei-Yu Chen, Yen-Cheng Liu, Zsolt Kira, Yu-Chiang Frank Wang, and Jia-Bin Huang. A closer look at few-shot classification. In *International Conference on Learning Representations*, 2019.
- Jia Deng, Wei Dong, Richard Socher, Li-Jia Li, Kai Li, and Li Fei-Fei. Imagenet: A large-scale hierarchical image database. In *2009 IEEE conference on computer vision and pattern recognition*, pages 248–255. Ieee, 2009.
- Andre Esteva, Brett Kuprel, Roberto A Novoa, Justin Ko, Susan M Swetter, Helen M Blau, and Sebastian Thrun. Dermatologist-level classification of skin cancer with deep neural networks. *Nature*, 542(7639):115, 2017.
- Li Fei-Fei, Rob Fergus, and Pietro Perona. One-shot learning of object categories. *IEEE transactions on pattern analysis and machine intelligence*, 28(4):594–611, 2006.
- Chelsea Finn, Pieter Abbeel, and Sergey Levine. Model-Agnostic Meta-Learning for Fast Adaptation of Deep Networks. *ICML*, March 2017. URL <http://arxiv.org/abs/1703.03400>. arXiv: 1703.03400.
- Jerome Friedman, Trevor Hastie, and Robert Tibshirani. *The elements of statistical learning*, volume 1. Springer series in statistics New York, 2001.
- Kaiming He, Xiangyu Zhang, Shaoqing Ren, and Jian Sun. Deep residual learning for image recognition. In *Proceedings of the IEEE conference on computer vision and pattern recognition*, pages 770–778, 2016.
- Nathan Hilliard, Lawrence Phillips, Scott Howland, Artëm Yankov, Courtney D Corley, and Nathan O Hodas. Few-shot learning with metric-agnostic conditional embeddings. *arXiv preprint arXiv:1802.04376*, 2018.
- Geoffrey Hinton, Oriol Vinyals, and Jeff Dean. Distilling the knowledge in a neural network. *arXiv preprint arXiv:1503.02531*, 2015.
- Diederik P Kingma and Jimmy Ba. Adam: A method for stochastic optimization. *arXiv preprint arXiv:1412.6980*, 2014.
- Mehmet Koç and Atalay Barkana. Application of linear regression classification to low-dimensional datasets. *Neurocomputing*, 131:331–335, 2014.
- Gregory Koch, Richard Zemel, and Ruslan Salakhutdinov. Siamese neural networks for one-shot image recognition. In *ICML deep learning workshop*, volume 2, 2015.
- Brenden Lake, Ruslan Salakhutdinov, Jason Gross, and Joshua Tenenbaum. One shot learning of simple visual concepts. In *Proceedings of the Annual Meeting of the Cognitive Science Society*, volume 33, 2011.
- Brenden M Lake, Ruslan Salakhutdinov, and Joshua B Tenenbaum. Human-level concept learning through probabilistic program induction. *Science*, 350(6266):1332–1338, 2015.
- Imran Naseem, Roberto Togneri, and Mohammed Bennamoun. Linear regression for face recognition. *IEEE transactions on pattern analysis and machine intelligence*, 32(11):2106–2112, 2010.
- Boris Oreshkin, Pau Rodríguez López, and Alexandre Lacoste. Tadam: Task dependent adaptive metric for improved few-shot learning. In *Advances in Neural Information Processing Systems*, pages 721–731, 2018.
- Adam Paszke, Sam Gross, Soumith Chintala, Gregory Chanan, Edward Yang, Zachary DeVito, Zeming Lin, Alban Desmaison, Luca Antiga, and Adam Lerer. Automatic differentiation in pytorch. 2017.

- Siyuan Qiao, Chenxi Liu, Wei Shen, and Alan L Yuille. Few-shot image recognition by predicting parameters from activations. In *Proceedings of the IEEE Conference on Computer Vision and Pattern Recognition*, pages 7229–7238, 2018.
- Sachin Ravi and Hugo Larochelle. Optimization as a model for few-shot learning. *ICLR*, page 11, 2017.
- David Silver, Aja Huang, Chris J Maddison, Arthur Guez, Laurent Sifre, George Van Den Driessche, Julian Schrittwieser, Ioannis Antonoglou, Veda Panneershelvam, Marc Lanctot, et al. Mastering the game of go with deep neural networks and tree search. *nature*, 529(7587):484, 2016.
- Christian Simon, Piotr Koniusz, and Mehrtash Harandi. Projective subspace networks for few-shot learning, 2019. URL <https://openreview.net/forum?id=rkzfuia9F7>.
- Jake Snell, Kevin Swersky, and Richard S. Zemel. Prototypical Networks for Few-shot Learning. *arXiv:1703.05175 [cs, stat]*, March 2017. URL <http://arxiv.org/abs/1703.05175>. arXiv: 1703.05175.
- Flood Sung, Yongxin Yang, Li Zhang, Tao Xiang, Philip HS Torr, and Timothy M Hospedales. Learning to compare: Relation network for few-shot learning. In *Proceedings of the IEEE Conference on Computer Vision and Pattern Recognition*, pages 1199–1208, 2018.
- Oriol Vinyals, Charles Blundell, Timothy Lillicrap, Daan Wierstra, et al. Matching networks for one shot learning. In *Advances in neural information processing systems*, pages 3630–3638, 2016.
- Catherine Wah, Steve Branson, Peter Welinder, Pietro Perona, and Serge Belongie. The caltech-ucsd birds-200-2011 dataset. 2011.
- Chen Xing, Negar Rostamzadeh, Boris N. Oreshkin, and Pedro O. Pinheiro. Adaptive cross-modal few-shot learning. *CoRR*, abs/1902.07104, 2019. URL <http://arxiv.org/abs/1902.07104>.

Appendix A

Table 2: CUB dataset 5-way 1-shot classification accuracies with 95% confidence intervals for different methods and backbones. For each backbone, the best-performing method is highlighted.

| | Conv-4 | ResNet-10 | ResNet-34 |
|---------------------------|---------------------|---------------------|---------------------|
| MatchingNet | 61.16 ± 0.89 | 71.29 ± 0.90 | 71.44 ± 0.96 |
| ProtoNet | 51.31 ± 0.91 | 70.13 ± 0.94 | 72.03 ± 0.91 |
| RelationNet | 62.45 ± 0.98 | 68.65 ± 0.91 | 66.20 ± 0.99 |
| SubspaceNet (ours) | 59.05 ± 0.90 | 72.92 ± 0.90 | 73.74 ± 0.88 |

Table 3: CUB dataset 5-way 5-shot classification accuracies with 95% confidence intervals for different methods and backbones. For each backbone, the best-performing method is highlighted.

| | Conv-4 | ResNet-10 | ResNet-34 |
|---------------------------|---------------------|---------------------|---------------------|
| MatchingNet | 76.74 ± 0.67 | 83.75 ± 0.60 | 85.96 ± 0.52 |
| ProtoNet | 76.14 ± 0.68 | 85.70 ± 0.52 | 88.49 ± 0.46 |
| RelationNet | 78.98 ± 0.63 | 82.67 ± 0.61 | 84.13 ± 0.57 |
| SubspaceNet (ours) | 78.48 ± 0.65 | 87.45 ± 0.48 | 89.30 ± 0.45 |

Table 4: CUB dataset 5-way 10-shot classification accuracies with 95% confidence intervals for different methods and backbones. For each backbone, the best-performing method is highlighted.

| | Conv-4 | ResNet-10 | ResNet-34 |
|---------------------------|---------------------|---------------------|---------------------|
| MatchingNet | 79.27 ± 0.61 | 85.38 ± 0.54 | 89.03 ± 0.46 |
| ProtoNet | 81.77 ± 0.57 | 87.61 ± 0.44 | 90.35 ± 0.40 |
| RelationNet | 82.66 ± 0.56 | 84.96 ± 0.53 | 87.29 ± 0.46 |
| SubspaceNet (ours) | 83.02 ± 0.53 | 89.28 ± 0.41 | 91.46 ± 0.36 |

Table 5: miniImageNet 5-way 1-shot classification accuracies with 95% confidence intervals for different methods and backbones. For each backbone, the best-performing method is highlighted.

| | Conv-4 | ResNet-10 | ResNet-34 |
|---------------------------|---------------------|---------------------|---------------------|
| MatchingNet | 48.14 ± 0.78 | 54.49 ± 0.81 | 53.20 ± 0.78 |
| ProtoNet | 44.42 ± 0.84 | 51.98 ± 0.84 | 53.90 ± 0.83 |
| RelationNet | 49.31 ± 0.85 | 52.19 ± 0.83 | 52.74 ± 0.83 |
| SubspaceNet (ours) | 47.99 ± 0.80 | 54.83 ± 0.83 | 53.93 ± 0.81 |

Table 6: miniImageNet 5-way 5-shot classification accuracies with 95% confidence intervals for different methods and backbones. For each backbone, the best-performing method is highlighted.

| | Conv-4 | ResNet-10 | ResNet-34 |
|---------------------------|---------------------|---------------------|---------------------|
| MatchingNet | 63.28 ± 0.68 | 69.14 ± 0.69 | 70.36 ± 0.70 |
| ProtoNet | 65.15 ± 0.67 | 73.77 ± 0.64 | 75.14 ± 0.65 |
| RelationNet | 65.33 ± 0.70 | 69.97 ± 0.68 | 71.38 ± 0.68 |
| SubspaceNet (ours) | 66.41 ± 0.66 | 74.03 ± 0.68 | 75.62 ± 0.61 |

Table 7: miniImageNet 5-way 10-shot classification accuracies with 95% confidence intervals for different methods and backbones. For each backbone, the best-performing method is highlighted.

| | Conv-4 | ResNet-10 | ResNet-34 |
|---------------------------|------------------------------------|------------------------------------|------------------------------------|
| MatchingNet | 67.47 \pm 0.64 | 74.63 \pm 0.62 | 73.88 \pm 0.65 |
| ProtoNet | 72.01 \pm 0.67 | 78.92 \pm 0.54 | 79.62 \pm 0.55 |
| RelationNet | 70.27 \pm 0.63 | 75.69 \pm 0.61 | 75.40 \pm 0.62 |
| SubspaceNet (ours) | 72.69 \pm 0.61 | 80.08 \pm 0.57 | 80.42 \pm 0.53 |